

Dynamical Behaviour of Plates Subjected to a Flowing Fluid

Y. KERBOUA AND A.A. LAKIS

Mechanical Engineering Department

École Polytechnique of Montreal

C.P. 6079, Succursale Centre-ville, Montreal, Quebec, H3C 3A7,
CANADA

Abstract: - In this paper we describe the development of a fluid-solid finite element to model plates subjected to flowing fluid under various boundary conditions. The mathematical model for the structure is developed using a combination of the finite element method and Sanders' shell theory. The membrane displacement field is approximated by bilinear polynomials and the transversal displacement by an exponential function. Fluid pressure is expressed by inertial, Coriolis and centrifugal fluid forces. Bernoulli's equation for the fluid-solid interface and partial differential equation of potential flow are applied to calculate the fluid pressure. Calculated results are in agreement with other analytical theories.

Key-Words: - Vibration, Finite element, Plates, Potential flow, Fluid-structure interaction.

1. Introduction

Systems of plates subjected to fluid flow are often found in contemporary industries such as nuclear reactors and aerospace. Generally these industries require high rates of fluid flow and low plate thicknesses. Under these conditions, if the length of the plates is excessive the structure becomes very susceptible to failure. Earlier works in this field were carried out on the engineering test reactor (ETR) systems consisting of many thin plates stacked in parallel with narrow channels between the plates to let coolant flow through. Miller [7] was the first to present a theoretical analysis predicting the critical flow velocity for divergence. Rosenberg et al. [8] have formulated a dynamic model describing the motion of a fuel plate in a parallel plate assembly. They found that a good agreement exists between the results of dynamical model and that of neutral equilibrium used by Miller [7]. Three parallel plate assemblies were tested by Groninger et al. [1] to investigate the flow induced deflections of the individual plates. The model showed that adjacent plates always move in opposite directions at high flow rates. Weaver et al. [11] studied the dynamic behaviour of a single flat plate, one side of which is exposed to high velocity flow of a heavy fluid such as water. More recently, Kim and Davis [4] developed an analytical model of a system of thin rectangular flat plates. Their model was used to investigate static and dynamic instabilities of the system. Guo and Paidoussis [2] have conducted a theoretical study of the hydro-elastic instabilities of

rectangular parallel-plate assemblies. The purpose of this paper is to develop a solid-fluid finite element to study the dynamic response of rectangular plate subjected to potential flow. This solid-fluid finite element permits us to obtain the low as well as the high frequencies of fluid-structure systems with precision for any combination of boundary conditions without changing the displacement field. This element is applied to simulate a number of plates and set of parallel plates subjected to flowing fluid. The mathematical model for the structure is developed using a combination of the finite element method and Sanders' shell theory. The velocity potential and Bernoulli's equation are adopted to express the fluid pressure acting on the structure.

2. Solid finite element

The solid finite element is shown in Fig. 1, it is a portion of a flat plate with a thickness h and four nodes (i, j, k, l). Each node has six degrees of freedom that represent the in-plane and out-of-plane displacement components and their spatial derivatives.

2.1 Displacement functions

The approximation of transversal displacement by exponential function and the membrane displacements by bilinear polynomials was justified when we developed the fluid-solid finite element [3]. The displacement field is expressed as:

$$U(x, y, t) = C_1 + C_2 \frac{x}{A} + C_3 \frac{y}{B} + C_4 \frac{xy}{AB} \quad (1.a)$$

$$V(x, y, t) = C_5 + C_6 \frac{x}{A} + C_7 \frac{y}{B} + C_8 \frac{xy}{AB} \quad (1.b)$$

$$W(x, y, t) = \sum_{j=9}^{24} C_j e^{i\pi \left(\frac{x}{A} + \frac{y}{B} \right)} e^{i\omega t} \quad (1.c)$$

where U and V represent the in-plane displacement components of the middle surface in X and Y directions, respectively, W is the transversal displacement of the middle surface, A and B are the plate dimensions in X and Y directions, “ ω ” is the natural frequency of the plate (rad/sec), “ i ” is a complex number and C_j are unknown constants;

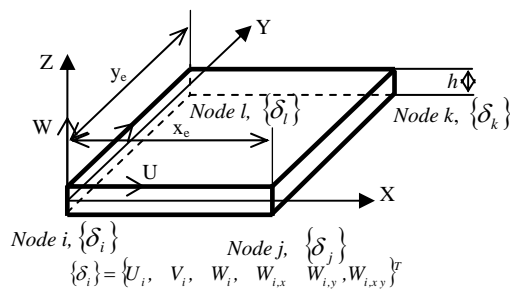


Fig. 1: Geometry and displacement field

Eq. (1.c) can be developed in Taylor's series as follows [3]:

$$\begin{aligned} W(x, y, t) = & C_9 + C_{10} \frac{x}{A} + C_{11} \frac{y}{B} + C_{12} \frac{x^2}{2A^2} + C_{13} \frac{xy}{AB} + C_{14} \frac{y^2}{2B^2} + \\ & C_{15} \frac{x^3}{6A^3} + C_{16} \frac{x^2y}{2A^2B} + C_{17} \frac{xy^2}{2AB^2} + C_{18} \frac{y^3}{6B^3} + C_{19} \frac{x^3y}{6A^3B} + \\ & C_{20} \frac{x^2y^2}{4A^2B^2} + C_{21} \frac{xy^3}{6AB^3} + C_{22} \frac{x^3y^2}{12A^3B^2} + C_{23} \frac{x^2y^3}{12A^2B^3} + C_{24} \frac{x^3y^3}{36A^3B^3} \end{aligned} \quad (2)$$

We can write the displacements, U , V and W in matrix form as,

$$\{U, V, W\}^T = [R]\{C\} \quad (3)$$

where $[R]$ is a (3x24) matrix in which the components are the x and y terms of Eq. (1.a, 1.b and 2) without the unknown constants [3] and $\{C\}$ is the vector for the unknown constants. The components of this last vector can be determined using the twenty-four degrees of freedom presented for a plate element as shown in Fig. 1. The displacement vector of each element is given as:

$$\{\delta\} = \left\{ \{\delta_i\}^T, \{\delta_j\}^T, \{\delta_k\}^T, \{\delta_l\}^T \right\}^T \quad (4)$$

Each node ‘ i ’, possesses a nodal displacement vector composed of the following terms:

$$\{\delta_i\} = \{U_i, V_i, W_i, W_{i,x}, W_{i,y}, W_{i,xy}\}^T \quad (5)$$

By introducing Eqs. (1.a, 1.b and 2) into relation (4), the elementary displacement vector can be defined as function of nodal displacement. The displacement field may be described by:

$$\{U, V, W\}^T = [R][A]^{-1}\{\delta\} = [N]\{\delta\} \quad (6)$$

where matrix $[N]$ of order (3 × 24) is the shape function of the finite element and the terms of matrix $[A]^{-1}$ are given in reference [3].

2.2. Kinematics Relations

Introducing the displacement components into the deformation-displacement relationships given in [9] yields to the following equation that describes the deformation vector as function of nodal displacements.

$$\{\varepsilon\} = [Q][A]^{-1}\{\delta\} = [B]\{\delta\} \quad (7)$$

where matrix $[Q]$ of order (6 × 24) is given in Appendix.

The stress-strain relationship of an isotropic rectangular plate is defined as follows:

$$\{\sigma\} = [P][B]\{\delta\} \quad (8)$$

where $[P]$ is the elasticity matrix for an isotropic plate [3].

Using the procedure of the classical finite element, one obtains the mass and stiffness matrices for a typical element:

$$[k_s]^e = [A]^{-1} \int_0^{y_e} \int_0^{x_e} [Q]^T [P] [Q] dx dy [A]^{-1} \quad (9.a)$$

$$[m_s]^e = \rho_s h [A]^{-1} \int_0^{y_e} \int_0^{x_e} [R]^T [R] dx dy [A]^{-1} \quad (9.b)$$

where x_e and y_e are dimensions of an element according to the X and Y coordinates, respectively.

3. Fluid-solid interaction

The fluid pressure acting upon the structure is generally expressed as a function of out-of-plane displacement and its derivatives i.e. velocity and acceleration. These three terms are respectively known as the centrifugal, Coriolis and inertial forces [10].

The fluid matrices will be combined with solid matrices as follows:

$$[[M_s] - [M_f]]\{\ddot{\delta}_T\} + [[C_s] - [C_f]]\{\dot{\delta}_T\} + [[K_s] - [K_f]]\{\delta_T\} = \{0\} \quad (10)$$

where $[M_s]$, $[C_s]$ and $[K_s]$ are the global matrices of mass, damping and rigidity of the elastic plate, $[M_f]$, $[C_f]$ and $[K_f]$ represent the inertial, Coriolis and centrifugal forces of potential flow and $\{\delta_T\}$ is the global displacement vector.

3.1. Fluid-solid finite element

The fluid-solid model is developed based on the following hypotheses: (i) the fluid flow is potential; (ii) vibration is linear; (iii) the fluid mean velocity distribution (U_x) is constant across a plate section and (iv) the fluid is incompressible. Taking account of these assumptions, the velocity potential must satisfy the Laplace equation. This relation is expressed in the Cartesian system by:

$$\phi_{,xx} + \phi_{,yy} + \phi_{,zz} = 0 \quad (11)$$

where ϕ is the potential function. The Bernoulli equation is given by:

$$\dot{\phi} + V_r^2/2 + P/\rho_f|_{z=0} = 0 \quad (12)$$

where P is the fluid pressure, V_r is the fluid velocity and ρ_f is the fluid density.

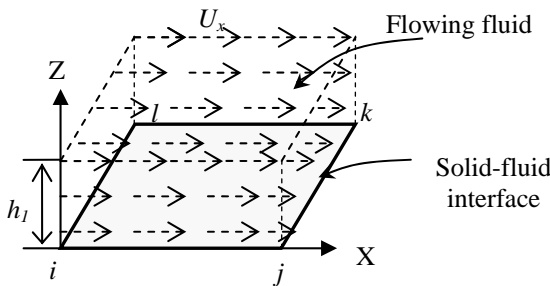


Fig. 2: Fluid-solid finite element

The components of fluid velocity along X, Y, Z directions, respectively are defined by:

$$V_x = U_x + \phi_{,x} \quad V_y = \phi_{,y} \quad V_z = \phi_{,z} \quad (13)$$

where U_x is the mean velocity of fluid in the x-direction. Introducing Eq. (13) into Eq. (12) and neglecting the nonlinear terms we can write the dynamic pressure at the solid-fluid interface as follows (see Fig. 2):

$$P|_{z=0} = -\rho_f \left(\dot{\phi} + U_x \phi_{,x} \right)|_{z=0} \quad (14)$$

The impermeability condition ensures contact between the shell and the fluid. This should be

$$\phi_{,z}|_{z=0} = (\dot{w} + U_x w_{,x}) \quad (15)$$

If we assume that:

$$\phi(x, y, z, t) = F(z)S(x, y, t) \quad (16)$$

where $F(z)$ and $S(x, y, t)$ are two separate functions to be defined. One can use Eqs. (15) and (16) to develop the potential function as:

$$\phi(x, y, z, t) = \frac{F(z)}{dF(0)/dz} (\dot{w} + U_x w_{,x}) \quad (17)$$

The only unknown function in Eq. (17) is $F(z)$. By introducing Eq. (17) into Eq. (11), we obtain the following differential equation of second order:

$$F_{,zz} - \mu^2 F(z) = 0 \quad (18)$$

where: $\mu = \pi \sqrt{1/A^2 + 1/B^2}$

The solution of last equation is:

$$F(z) = A_1 e^{\mu z} + A_2 e^{-\mu z} \quad (19)$$

where A_1 and A_2 are unknown constants. By substituting Eq. (19) into (17) the potential function becomes:

$$\phi(x, y, z, t) = \frac{(A_1 e^{\mu z} + A_2 e^{-\mu z})}{dF(0)/dz} (\dot{w} + U_x w_{,x}) \quad (20)$$

3.1.1. Fluid-solid finite element subject to flowing fluid with infinite level of fluid

When the flowing fluid height on and/or under the plate (h_1 and/or h_2) is infinite (see Fig. 2), we assume that very far from the plate the potential is null, this boundary condition is written as follows:

$$\phi = 0 \quad Z \rightarrow \pm\infty \quad (21)$$

In order to avoid an infinite potential, the constant A_1 of Eq. (20) must be null. Eq. (15) permits us to calculate the second constant A_2 . Using Eqs (20) and (14) the pressure function can be expressed as:

$$P = \frac{\rho_f}{\mu} [\ddot{w} + 2U\dot{w}_{,x} + U_x^2 w_{,xx}] = Z_{f1} [\ddot{w} + 2U\dot{w}_{,x} + U_x^2 w_{,xx}] \quad (22)$$

3.1.2. Fluid-solid finite element subject to flowing fluid bounded by rigid wall

As shown in Fig. 3, fluid flows between a rigid wall and an elastic plate. This provides another boundary condition at $Z=h_1$. This boundary condition is adopted by Lamb [6] expressed by:

$$\phi_{,z}|_{z=h_1} = 0 \quad (23)$$

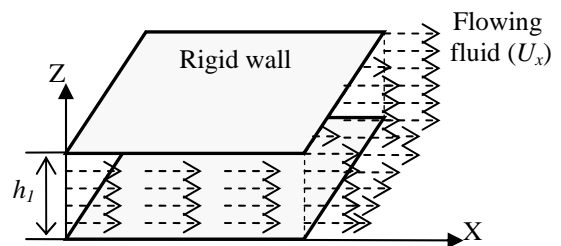


Fig. 3: Fluid solid finite element in contact with flowing fluid bounded by a rigid wall

Using Eqs. (15) and (23) we can calculate the constants A_1 and A_2 . The corresponding dynamic pressure becomes:

$$P = \frac{-\rho_f (e^{-2\mu h_1} + 1)}{\mu (e^{-2\mu h_1} - 1)} [\ddot{w} + 2U\dot{w}_{,x} + U_x^2 w_{,xx}] \quad (24)$$

or:

$$P = Z_{f2} [\ddot{w} + 2U\dot{w}_{,x} + U_x^2 w_{,xx}] \quad (25)$$

3.1.3. Fluid-solid finite element subject to flowing fluid bounded by elastic plate

When the fluid flows through two parallel elastic plates, two transverse vibration modes, in-phase and out-of-phase, should be considered.

In the case of in-phase mode the boundary condition at fluid limits $Z=h_1$ is expressed as follows [5]:

$$\left. \frac{\partial \phi}{\partial z} \right|_{z=h_1} = (\dot{W} + U_x W_{,x}) \quad (26)$$

Similarly, A_1 and A_2 can be calculated by introducing Eq. (20) into relations (15) and (26). The pressure function can be expressed as:

$$P = -\frac{\rho_f}{\mu} \left(\frac{2 - e^{-ih_1} - e^{ih_1}}{e^{ih_1} + e^{-ih_1}} \right) [\ddot{W} + 2U_x \dot{W}_{,x} + U_x^2 W_{,xx}] \quad (27)$$

or:

$$P = Z_{f3} [\ddot{W} + 2U_x \dot{W}_{,x} + U_x^2 W_{,xx}] \quad (28)$$

In the case of out-of-phase mode the boundary condition at $Z=h_1$ is expressed as follows [5]:

$$\phi_{,x} \Big|_{Z=h_1/2} = 0 \quad (29)$$

Here again, A_1 and A_2 can be calculated by using Eqs. (20, 29 and 15). The corresponding pressure is:

$$P = -\frac{\rho_f (e^{-ih_1} + 1)}{\mu (e^{-ih_1} - 1)} [\ddot{W} + 2U_x \dot{W}_{,x} + U_x^2 W_{,xx}] \quad (30)$$

or:

$$P = Z_{f4} [\ddot{W} + 2U_x \dot{W}_{,x} + U_x^2 W_{,xx}] \quad (31)$$

3.2 Calculation of fluid-induced force

The elementary vector of fluid-induced force is expressed by:

$$\{F\}^e = \int_A [N]^T \{P_v\} dS \quad (32)$$

where $[N]$ is defined in Eq. (6), $\{P_v\}$ is a tensor expressing the pressure applied by the fluid on the plate and S is the elementary fluid-structure interface area. By placing the matrix $[N]$ of Eq. (6) into Eq. (32), the element load vector becomes:

$$\{F\}^e = \int_A [[A]^{-1}]^T [R]^T \{P_v\} dS \quad (33)$$

The dynamic pressures of Eqs. (22, 25, 28 and 31) may be rewritten as:

$$P = Z_{fi} [\ddot{W} + 2U_x \dot{W}_{,x} + U_x^2 W_{,xx}] \quad (34)$$

where Z_{fi} ($i=1, 4$), depends on the boundary conditions (see Eqs. 22, 25, 28 and 31) and P is the only non-zero component in the pressure tensor $\{P_v\}$.

Substituting Eq. (1.c) into Eq. (34) the pressure expression becomes:

$$P = Z_{fi} [\ddot{W} + (2i\pi U_x/A) \dot{W} + (i^2 \pi^2 U_x^2/A^2) W] \quad (35)$$

The transversal displacement can be separated from Eq. (6) as follows:

$$\{0 \ 0 \ W\}^T = [R_f][A]^{-1} \{\delta\} \quad (36)$$

where $[R_f]$ is a (3x24) matrix obtained from matrix $[R]$ by neglecting the in-plane displacements U and V . Substituting (36) into (35), we obtain:

$$\{P_v\} = Z_{fi} [R_f][A]^{-1} \left(\begin{array}{l} \{\ddot{\delta}\} + (2i\pi U_x/A) \{\dot{\delta}\} + \\ (i^2 \pi^2 U_x^2/A^2) \{\delta\} \end{array} \right) \quad (37)$$

By combining Eqs. (33) and (37) the element load vector is given by the following relation:

$$\{F\}^e = Z_{fi} \left(\begin{array}{l} \int_A [[A]^{-1}]^T [R]^T [R_f][A]^{-1} \{\ddot{\delta}\} dS + \\ 2U_x \frac{i\pi}{A} \int_A [[A]^{-1}]^T [R]^T [R_f][A]^{-1} \{\dot{\delta}\} dS + \\ U_x^2 \frac{i^2 \pi^2}{A^2} \int_A [[A]^{-1}]^T [R]^T [R_f][A]^{-1} \{\delta\} dS \end{array} \right) \quad (38)$$

We can separate From Eq. (38) the added matrices induced by flowing fluid.

4. Eigenvalue problem

The global matrices mentioned in Eq. (10) are obtained by superimposing the matrices for each individual element. The eigenvalue problem is solved by means of the equation reduction technique. It may be written as:

$$\begin{bmatrix} 0 & [I] \\ [K]^{-1}[M] & [K]^{-1}[C] \end{bmatrix} - \Lambda [I] = 0 \quad (39)$$

with $\Lambda = 1/i\omega^2$ and $[I]$ is the identity matrix, where $[M] = [M_s] - [M_f]$, $[C] = [C_f]$, $[K] = [K_s] - [K_f]$ and $\{\delta_T\}$ is the global displacement vector.

5. Results and discussions

We present some calculations to test the solid-fluid model in the case of plates subjected to flowing fluid.

To put the results in the nondimensional form, the following parameters are defined

$$\psi = \frac{\rho_f B}{\rho_s h}, \quad \bar{\omega} = B^2 \sqrt{\frac{\rho_s h}{K}} \omega, \quad \bar{U} = B \sqrt{\frac{\rho_s h}{K}} U_x \quad (40)$$

where ψ is the mass ratio, $\bar{\omega}$ is the dimensionless frequency, and \bar{U} is the dimensionless velocity.

The first example is a thin plate clamped on two opposite edges (see Fig. 4) subjected to flowing fluid on its upper and lower surfaces. The fluid level (h_1 and/or h_2) is assumed to be infinite. The corresponding dynamic pressure would be twice the

pressure calculated in Eq. (22). The geometric ratios and dimensionless parameters for the structure are:
 $\psi = 0.93$, $h_1/A \rightarrow \infty$, $h_2/A \rightarrow \infty$, $A/B = 1$

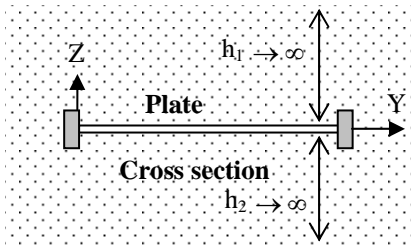


Fig. 4: Plate clamped on two opposite edges subjected to flowing fluid

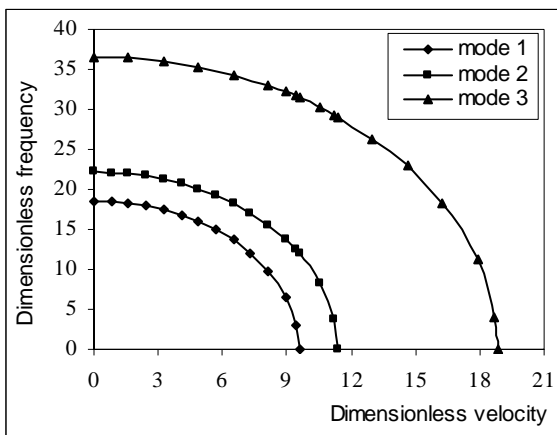


Fig. 5: Variation of frequency ω versus fluid velocity for plate clamped on two opposite edges.

Numerical results were used to plot the curves shown in Fig. 5. We note that the plate becomes increasingly vulnerable to static instability as the rate of flow increases. Beyond the critical velocity we expect the occurrence of a large deflection of the plate [4].

In order to investigate the boundary conditions effect on the critical velocity value, the same plate considered in the first example is studied again, but this time with the two opposite edges simply supported instead of the two clamped edges. The critical velocities corresponding to the three first modes are listed in table 1, it can be concluded that clamped plates are more stable than simply supported plates which is in good agreement with the observations of Kim and Davis [4].

We have also calculated the critical velocities corresponding to the first three modes in the case of cantilevered plate (fixed at leading edge) which has the same material and geometrical parameters as those of the two previous examples. We have compared in Table 1 the critical velocities of the

cantilevered plate with those of simply supported and clamped on two opposite edges plates. We conclude that the cantilevered plate is more vulnerable to static instability

Table 1: Dimensionless critical velocity (\bar{U}) of plates with various boundary conditions

Boundary conditions	$\bar{U} = B\sqrt{\rho_s h/K} U_x$		
	Mode 1	Mode 2	Mode 3
Clamped on two opposite edges (Fig. 4)	9.58	11.36	18.83
Simply supported on two opposite edges	4.22	6.98	15.83
Cantilevered plate	1.494	3.73	9.25

Parallel-plate assemblies consist of many thin plates stacked in parallel; between the plates there are narrow channels to let coolant flow through (see Fig. 6). All the plates have the same size and are uniformly distributed. When channel height is relatively low, kinetic energy travels through the fluid from one plate to another.

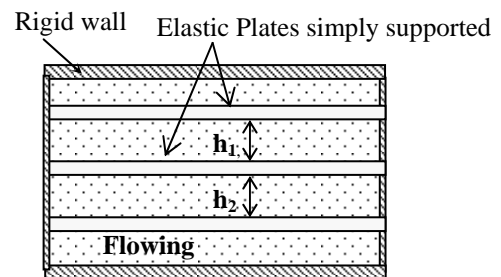


Fig. 6 Engineering test reactor (ETR) system subjected to flowing fluid

It has been proven that the dynamic behaviour of parallel-plate assemblies supported at two lateral walls can be sufficiently predicted using only one plate which vibrates in opposite directions relatively to its adjacent plates. This condition provides the lower critical velocity [2]. Miller [7] derived relations expressing the critical velocity of an engineering test reactor system. For the case of a flat plate simply supported on two opposite edges (see Fig. 6), the developed formula is:

$$U_{Miller} = \sqrt{5Eh^3 h_1 / (2\rho_f B^4 (1-\nu^2))} \quad (41)$$

where E is Young modulus, ρ_f is the fluid density, h_1 is the channel height, ν Poisson's coefficient, h is the plate thickness and B is the plate width.

Using our numerical model, we have calculated the out-of-phase vibrations of an internal plate (simply supported on its two opposite edges) from the parallel-plate assembly shown in Fig. 6. The corresponding dynamic pressure would be twice the pressure calculated in Eq. (31). Fig. 7 shows the variation of the dimensionless critical velocities of the first out-of-phase mode as function of channel height to plate length ratio computed by the present method and by Miller's analytical formula. By examining Fig. 7, it is clear that the critical velocity for a given plate increase by increasing the channel height.

In the same figure, we can see that at low fluid height a good agreement is found between the numerical and analytical results, but for high fluid levels we observe a considerable discrepancy, that can be explained by the fact that Miller's formula is derived specifically for parallel plate system with very low ratio (h_1/A). On the other hand, it is important to note that beyond certain fluid height, increasing ' h_1 ' or ' h_2 ' doesn't have any influence on the dynamic behaviour of plate subjected to a flowing fluid [4].

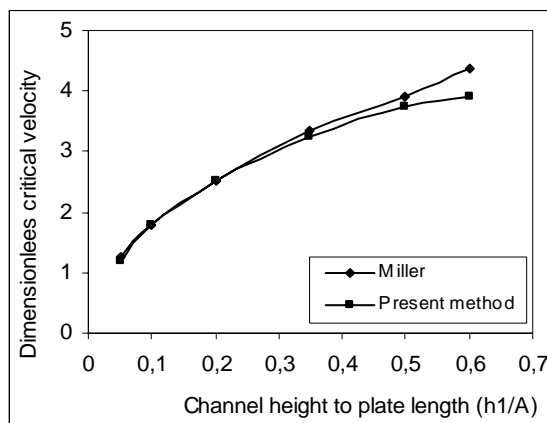


Fig. 7: Dimensionless critical velocity of an internal plate in (ETR) versus channel height to plate length ratio (h_1/A), $\psi = 0.93$, $A/B = 1$.

6. Conclusions

A solid-fluid finite element is developed for dynamic analysis of plates subjected to the dynamic pressure induced by potential flow. The structural mathematical model is developed based on a combination of the finite element method and Sanders' shell theory.

The fluid pressure is derived from a potential, it is function of acceleration, velocity and the transverse

displacement of the plate, respectively known as inertial, Coriolis and centrifugal effects.

The critical velocities calculated using our element agrees well with those obtained using the analytical formulas derived by Miller, especially for the low fluid heights.

References

- [1] R.D. Groninger, J.J. Kane, Flow induced deflections of parallel flat plates, Nuclear Science and Engineering, Vol.16, 1963, pp. 218-226.
- [2] C.Q. Guo, M.P. Paidoussis, Analysis of hydroelastic instabilities of rectangular parallel-plate assemblies. ASME, Pressure Vessels and Piping Division, Vol.389, 1999, 191-198.
- [3] Y. Kerboua, A.A. Lakis, M. Thomas L. Marcouiller, Hybrid method for vibration analysis of rectangular plates, Nuclear Engineering and Design Vol.237 No.8 2007, pp. 791-801.
- [4] G. Kim, D.C. Davis, Hydrodynamic instabilities in flat-plate-type fuel assemblies, Nuclear Engineering and Design Vol.158, No.1, 1995, pp. 1-17.
- [5] K.H. Jeong, G.H. Yoo, S.C. Lee, Hydroelastic vibration of two identical rectangular plates, Journal of Sound and Vibration, Vol.272, No.3-5, 2004. pp. 539-55.
- [6] H. Lamb, On the Vibrations of an Elastic Plate in Contact with Water. Proceedings of the Royal Society of London. Vol.98, No.690, 1920, pp. 205-216.
- [7] D.R. Miller, Critical flow velocities for collapse of reactor parallel-plate fuel assemblies, ASME, Journal of Engineering for Power Series A, Vol. 82, No.2, 1960, pp. 83-95.
- [8] G.S. Rosenberg, C.K. Youngdahl, A simplified dynamic model for the vibration frequencies and critical coolant flow velocities for reactor parallel plate fuel assemblies, Nuclear Science and Engineering, Vol.13, No.2, 1962, pp. 91-102.
- [9] J.L. Sanders, An improved first approximation theory for thin shell, 1959, NASA TR-24.
- [10] A. Selmane A.A. Lakis, Vibration analysis of anisotropic open cylindrical shells subjected to a flowing fluid, Journal of Fluids and Structures Vol.11, No.1, pp. 111-134.
- [11] D.S. Weaver, T. E. Unny, The hydroelastic stability of a flat plate. ASME, Series E, Journal of Applied Mechanics Vol.37 N3: 1970, pp. 823-27.